ARTICLE

ACS chemical biology

Structural Basis of the Radicicol Resistance Displayed by a Fungal Hsp90

Chrisostomos Prodromou[†], James M. Nuttall[‡], Stefan H. Millson[‡], S. Mark Roe[†], Tiow-Suan Sim[§], Doreen Tan[§], Paul Workman[¶], Laurence H. Pearl[†], and Peter W. Piper[‡,*]

[†]Section of Structural Biology, The Institute of Cancer Research, Chester Beatty Laboratories, 237 Fulham Road, London SW3 6JB, U.K., [‡]Department of Molecular Biology and Biotechnology, The University of Sheffield, Western Bank, Sheffield S10 2TN, U.K., [§]Department of Microbiology, Yong Loo Lin School of Medicine, National University of Singapore, 5 Science Drive 2, S117597, Singapore, and [¶]Cancer Research UK Centre for Cancer Therapeutics, The Institute of Cancer Research, Haddow Laboratories, 15 Cotswold Road, Sutton, Surrey SM2 5NG, U.K.

ABSTRACT Heat shock protein 90 (Hsp90) is a promising cancer drug target, as multiple oncogenic proteins are destabilized simultaneously when it loses its activity in tumor cells. Highly selective Hsp90 inhibitors, including the natural antibiotics geldanamycin (GdA) and radicicol (RAD), inactivate this essential molecular chaperone by occupying its nucleotide binding site. Often cancer drug therapy is compromised by the development of resistance, but a resistance to these Hsp90 inhibitors should not arise readily by mutation of those amino acids within Hsp90 that facilitate inhibitor binding, as these are required for the essential ATP binding/ATPase steps of the chaperone cycle and are tightly conserved. Despite this, the Hsp90 of a RAD-producing fungus is shown to possess an unusually low binding affinity for RAD but not GdA. Within its nucleotide binding site a normally conserved leucine is replaced by isoleucine, though the chaperone ATPase activity is not severely affected. Inserted into the Hsp90 of yeast, this conservative leucine to isoleucine substitution recreated this lowered affinity for RAD *in vitro*. It also generated a substantially enhanced resistance to RAD *in vivo*. Co-crystal structures reveal that the change to isoleucine is associated with a localized increase in the hydration of an Hsp90-bound RAD but not GdA. To the best of our knowledge, this is the first demonstration that it is possible for Hsp90 inhibitor resistance to arise by subtle alteration to the structure of Hsp90 itself.

Hsp90 orchestrates a multistage chaperone cycle, essential for the final folding, maturation, stabilization, and localization events of a diverse set of important proteins in eukaryotic cells. Among these "client" proteins of Hsp90 are many of the key activities determining carcinogenesis, such as ERBB2, c-RAF, CDK4, AKT/PKB, steroid receptors, mutant p53, HIF-1, survivin and telomerase (*1, 2*). When the function of the Hsp90 chaperone is lost, several of these oncogenic proteins are, in a concerted manner, inactivated and targeted for degradation. In this way, Hsp90 inhibitor drugs are able to cause the combinatorial depletion of many cancer-causing pathways and a modulation of all the hallmark traits of malignancy (*1, 3–5*). Importantly, these drugs display a high selectivity for cancer versus normal cells (*6, 7*) and a therapeutic activity at doses that are well tolerated in cancer patients (*8*).

Hsp90 is a GHKL-family ATPase, the binding and hydrolysis of ATP by this essential molecular chaperone being integral to its capacity to perform the events of client protein activation. Highly selective Hsp90 inhibitors occupy the ATP binding site, thereby preventing the progression of the chaperone cycle. There are two modes of inhibitor binding, exemplified by the interactions of the natural antibiotics geldanamycin (GdA) and radicicol (RAD). Hsp90 drugs that are GdA derivatives, as well as purine and 4,5-diaryisoxazole resorcinol inhibitors based on the interactions of RAD, are now in cancer clinic trials (*1–3, 8–10*). Drug therapy is often eventually compromised by the development of drug resistance. Whether it is possible for an increased resistance to Hsp90 inhibitors to arise through mutation to Hsp90

*Corresponding author, peter.piper@sheffield.ac.uk.

Received for review December 8, 2008 and accepted February 23, 2009.

Published online February 23, 2009

10.1021/cb9000316 CCC: $40.75

TABLE 1. Properties of the purified wild-type and mutant forms of *H. fuscoatra* Hsp90 and yeast Hsp82 investigated in this study

Hsp90	ATPase activity (K_{cat}, min^{-1})	K_d[a] AMPPNP (μM)	K_d[a] RAD (nM)	K_d[a] GdA (μM)
H. fuscoatra wild-type	0.48	104 ± 3.6	92 ± 0.014 93 ± 0.010	0.67 ± 0.03
H. fuscoatra I33L,I34V mutant	0.48	125.6 ± 6.5	6 ± 0.002	0.57 ± 0.05
Yeast Hsp82 wild-type	0.88[b]	111 ± 6.4	16 ± 0.003	2.9 ± 0.32
Yeast L34I,I35V mutant	0.92	80.3 ± 4.12	90 ± 0.007	1.27 ± 0.09 1.4 ± 0.16
Yeast L34I mutant	0.84[b]	67.5 ± 17.3	81 ± 0.11 76 ± 0.001	n.d.
Yeast I35V mutant	0.79	134 ± 5.2	14 ± 0.002 11 ± 0.002	n.d.

[a]Full data sets for these ITC experiments are presented in Supplementary Table S1. [b]The Km values for ATP binding by wild-type and L34I mutant Hsp82 were determined to be 500 and 420 nM, respectively.

itself is still unknown, as studies to date have only shown an increased sensitivity to these inhibitors with defects in the Hsp90 chaperone machine (*11–13*). We reasoned that, should nature have evolved an inhibitor-resistant form of Hsp90, it would most probably be found in those microbes that make Hsp90-targeting antibiotics, so as to protect these organisms against their own antibiotic production. We have therefore analyzed the Hsp90 of *Humicola fuscoatra*, a fungus that produces RAD (*14*). As described in this Article, this *H. fuscoatra* Hsp90 binds RAD less tightly than normal and contains a conservative amino acid substitution in the ATP-binding pocket. The latter, when introduced into the native Hsp90 of yeast, recreates this lowered affinity for RAD *in vitro* and generates substantial resistance to RAD *in vivo*. Crystal structures reveal that this sequence change alters the hydration of Hsp90-coordinated RAD.

RESULTS AND DISCUSSION

***Humicola fuscoatra* Hsp90 Exhibits an Unusually Low Binding Affinity for RAD.** Most fungal species have just a single, cytosolic form of Hsp90 (*15*). We sequenced the 2169bp of genomic DNA that encodes this Hsp90 in *H. fuscoatra* (GenBank Accession EU747829). The encoded chaperone has a high protein sequence identity with the Hsp90s of yeasts, as well as the human isoforms of cytosolic Hsp90 that are important cancer drug targets (75% *H. fuscoatra* Hsp90 to *Saccharomyces cerevisiae* Hsp90; 63–65% *H. fuscoatra* Hsp90 to human Hsp90α/Hsp90β).

To determine whether this *H. fuscoatra* Hsp90 exhibits any unusual properties of inhibitor binding, we prepared it in a bacterially expressed, purified form and then compared its properties to those of the well-studied Hsp90 of yeast (Hsp82 isoform of *S. cerevisiae*) (see Methods). Measuring the *in vitro* ATPase activity, the very slow ATP turnover rate intrinsic to purified Hsp82 (*16*) was found to be slightly lower in the case of the *H. fuscoatra* Hsp90 (Table 1). Determining binding affinities for RAD, GdA, and a non-hydrolyzable derivative of ATP (AMPPNP) by isothermal titration calorimetry (ITC), the *H. fuscoatra* Hsp90 was found to have an affinity for RAD 5.7-fold lower than that of yeast Hsp82. In contrast, both Hsp90s exhibited similar binding affinities for GdA and AMPPNP (Table 1).

Change to a Normally Conserved Amino Acid Found in *H. fuscoatra* Hsp90 Confers RAD Resistance When Introduced into the Hsp82 of Yeast. High-resolution crystal structures have revealed in atomic detail the interactions made by ATP, GdA, and RAD, as well as various Hsp90 inhibitor drugs, when these are bound within the N-terminal domain of the yeast or the human Hsp90 (*9, 17–22*). The amino acid residues facilitating these interactions are all highly conserved in Hsp90-family pro-

teins from bacteria to man (*15*). Indeed their mutation would generally be predicted to severely compromise the ATP binding or ATP hydrolysis steps that are so essential for the actions of this chaperone *in vivo*. With regard to the residues interacting with RAD, the only unusual feature of *H. fuscoatra* Hsp90 is the presence of an isoleucine (I33) instead of the normal leucine immediately after the glutamate (E32) that catalyzes the intrinsic ATPase reaction of Hsp90 (*23*). RAD, purine, and resorcinol inhibitors normally hydrogen bond, *via* a water molecule, to the polypeptide backbone at this leucine position (*9, 19–22*). Also, whereas the residue that immediately follows this leucine is isoleucine in most Hsp90 sequences, I33 is followed by valine (V34) in the *H. fuscoatra* Hsp90.

To investigate the effects of this L33I,I34V (LI to IV) sequence change by biological assay, we initially constructed yeast strains that express as their sole Hsp90 either a wild-type or a I33L,V34I double mutant form of this heterologous *H. fuscoatra* Hsp90 or the wild-type or a L34I,I35V double mutant form of the native yeast Hsp82. To help ensure that the levels of Hsp90 in these strains would approximate those that are normally present in yeast, each Hsp90 was expressed as a single copy gene under the control of the *HSC82* gene promoter, the promoter that drives most of the Hsp90 expression in unstressed, wild-type *S. cerevisiae* (*24*) (see Methods).

These four yeast strains displayed similar Hsp90 expression levels and growth at 28 °C (Figure 1, panels a and b). Agar growth analysis of their resistances to GdA and RAD indicated that all four were exhibiting a high GdA resistance (yeast is generally more resistant to GdA than RAD (*25*)) but that the LI to IV mutation of the native Hsp82 had increased the resistance of the cells to RAD (Figure 1, panel c). The yeast expressing the wild-type form of *H. fuscoatra* Hsp90 also displayed a moderate degree of RAD resistance during agar but not liquid growth (Figure 1, panels c and d). However, with the IV to LI mutation of this *H. fuscoatra* Hsp90, a change that reverts these two residues to those present in the wild-type, native Hsp82 of yeast, the yeast was rendered hypersensitive to RAD (Figure 1, panel c and d). The two yeasts expressing different forms of the heterologous *H. fuscoatra* Hsp90 were also found to be appreciably stress-sensitive (displaying temperature and lithium sensitivity, as well as a compromised capacity to induce the heat shock response at high temperature; see Supplementary Figure S1). Since stress sensitivity in mutant strains can be associated with a sensitization to diverse drugs, we continued our investigations of *in vivo* mutational changes using Hsp82, the Hsp90 native to yeast.

We next analyzed the effects of the L34I and I35V single mutations in this Hsp82, to see if either of these alone could confer the RAD resistance. These single mutant forms were expressed to similar levels (Figure 1, panel a); furthermore, neither affected the growth of the yeast at 28 °C, rendered the cells noticeably stress-sensitive, or affected the heat shock response (Figure 1, panel b; Supplementary Figure S1). Measurements of the effects of RAD on liquid medium growth revealed that the L34I single mutation was conferring the *in vivo* RAD resistance observed previously for the L34I,I35V double mutant (Figure 1, panel d). I35V in contrast exerted the opposite effect, acting to render the cells more sensitive to RAD inhibition (Figure 1, panel d). This analysis revealed therefore that L34I mutation of the native Hsp82 in yeast is alone sufficient to confer a substantial degree of RAD resistance *in vivo*.

Leucine to Isoleucine Change Weakens RAD Binding to the Purified Chaperone. Table 1 shows the influences of these same amino acid substitutions on ligand binding, measured by ITC. Both L34I,I35V double mutation and L34I single mutation of Hsp82 reduced the affinity of this chaperone for RAD, to the level displayed by the wild-type Hsp90 of *H. fuscoatra*. In contrast, the I35V single mutation of Hsp82 was without any major effect (Table 1). Conversely, the reciprocal I33L,V34I double mutation in the *H. fuscoatra* Hsp90 increased the affinity for RAD to the level displayed by the native Hsp82 of yeast (Table 1). The *in vitro* affinities of these purified Hsp90s for RAD are therefore consistent with how, when expressed as the sole Hsp90 of yeast, these forms of the chaperone influence RAD resistances *in vivo* (Figure 1, panel d). Both L34I,I35V mutation of Hsp82, as well as the reciprocal I33L,V34I mutation in the *H. fuscoatra* Hsp90, exerted much smaller effects on the bindings of GdA and AMPPNP (Table 1). Furthermore, L34I single mutation of Hsp82 was without any major effect on either the intrinsic ATPase activity or the K_m for ATP of the purified chaperone (Table 1).

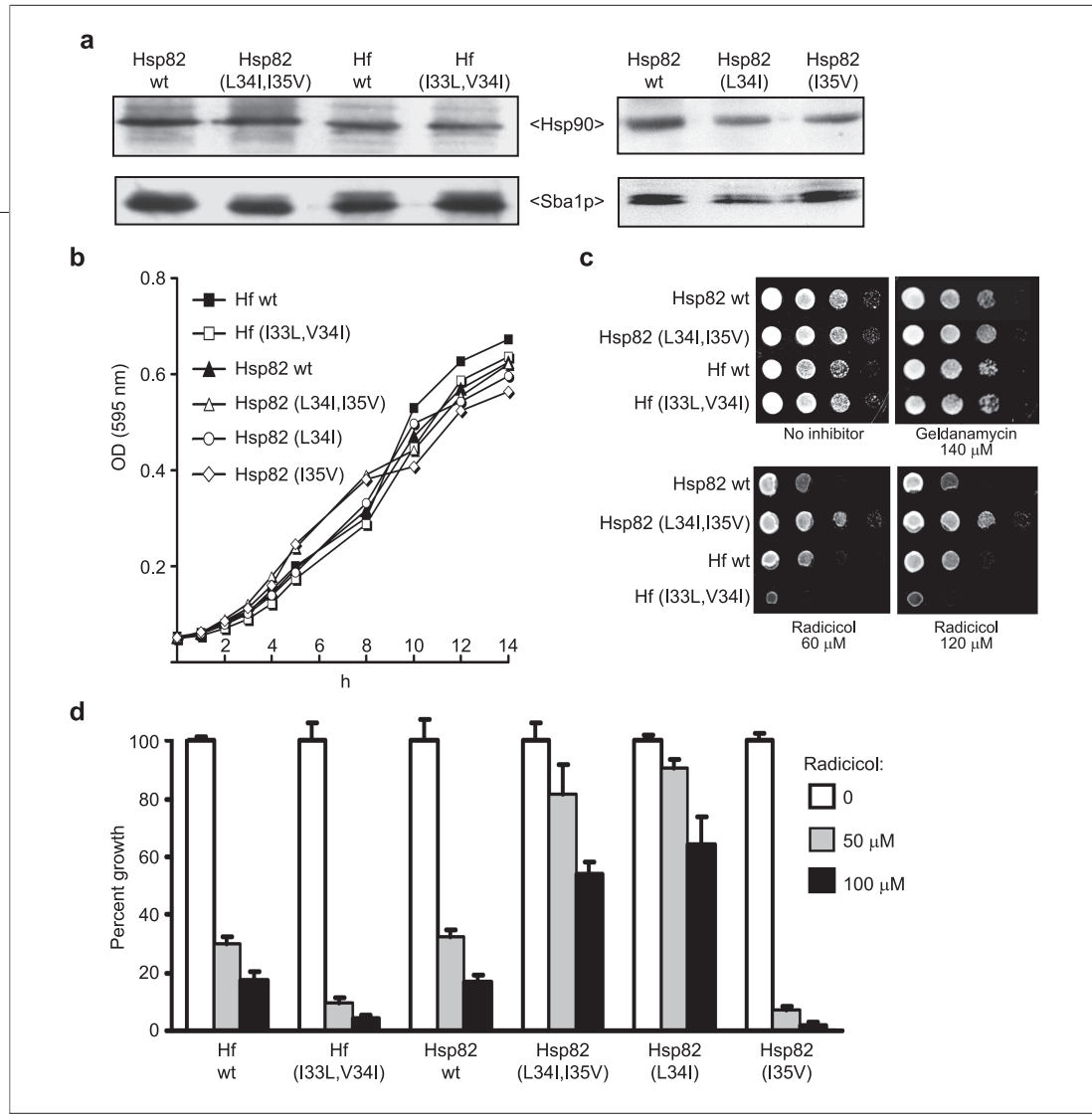

Figure 1. Expression of variant Hsp90s in yeast reveals the amino acid immediately after the catalytic glutamate determines RAD resistance. a) Analysis of Hsp90 level in strains expressing either the wild-type (wt), L34I,I35V double mutant, L34I or I35V single mutant yeast Hsp82 and also wild-type or I33L,V34I mutant *H. fuscoatra* (Hf) Hsp90. Samples (20 μg) of total cell protein were fractionated and then Western blotted, and the blots were probed with polyclonal rabbit antisera raised against yeast Hsp90 or Sba1p, the latter a loading control. b) Growth of these strains on synthetic defined (SD) liquid medium at 28 °C. c)Ten-fold serial dilutions of overnight cultures, gridded onto YPDA agar and then grown for 3 d at 30 °C in the presence of the indicated level of RAD or GdA. d) Final cell density after culture for 16 h at 28 °C in SD medium either in the absence or in the presence of 50 or 100 μM RAD (mean and standard deviation of six replicate growths, OD_{595nm} expressed as a percentage of the DMSO controls, the latter all displaying <8% inhibition of growth).

Co-crystal Structures Reveal How the Leucine to Isoleucine Substitution Generates an Altered Hydration of RAD and ADP but Not GdA in Association with Hsp82. Next, high-resolution crystal structures were determined for RAD, GdA, and ADP bound within a L34I, I35V mutant form of the N-terminal domain subfragment (amino acid residues 1−221) of yeast Hsp82 (see Methods and Supplementary Table S2). These were then compared with the previously determined structures of the same ligands interacting with the wild-type form of this fragment (*17, 19*) (Figure 2 and Figure 3). Apart from the structural changes implicit from the LI to IV mutation, the structure of the LI to IV N-terminal domain was essentially that of the wild-type N-terminal domain of Hsp82. Furthermore, the LI to IV sequence change did not noticeably affect either the conformations or the chemical space occupied by either RAD, GdA, or ADP, bound within this N-terminal domain (Figure 2 and Figure 3; Supplementary Figure S2). Instead, it was apparent that the leucine to isoleucine side-chain substitution at position 34 had caused the slight enlargement of a hydrophobic pocket, which in the case of the RAD/LI to IV and ADP/LI to IV Hsp82 co-crystal structures had allowed three additional water molecules to enter and establish a new subnetwork of hydrogen bonds (hydrogen bonds to the side-chain hydroxyl of

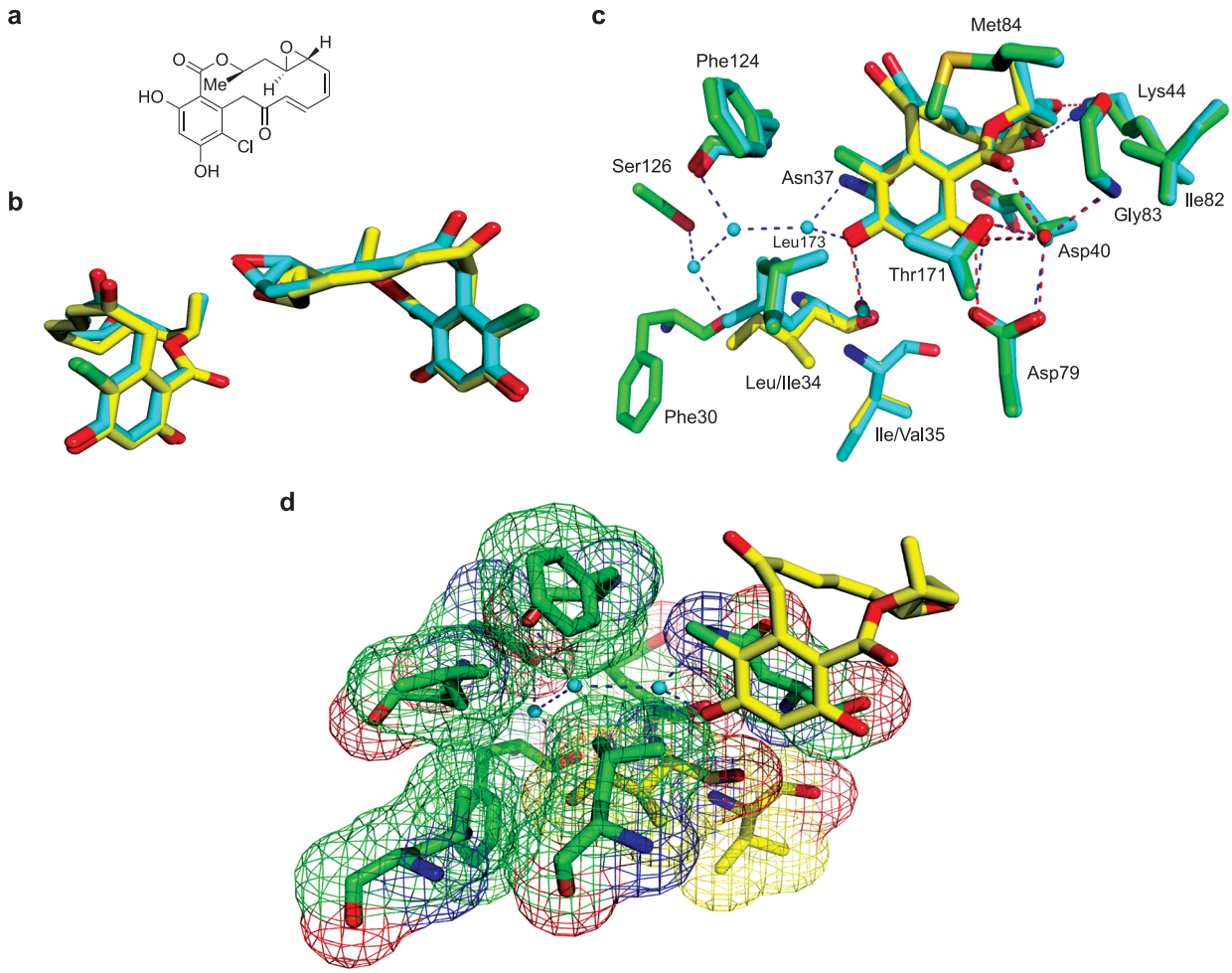

Figure 2. Conformation and binding interactions of RAD within the N-terminal domain of wild-type and L34I,I35V mutant yeast Hsp82. a) The chemical structure of RAD. b) Two orthogonal views of superimpositions of RAD from the wild-type and LI to IV mutant Hsp82 co-crystal structures, revealing that RAD occupies a nearly identical space in the ATP-binding site of the wild-type (cyan) and LI to IV mutant (yellow) Hsp82. c) PyMol diagrams showing RAD (wild-type structure in cyan and LI to IV mutant structure in yellow). Amino acid residues from the wild-type Hsp82 are shown in cyan while those from the LI to IV mutant protein are in green, except for the residues representing the LI to IV mutations, which are in yellow. Hydrogen bonds are shown as red (wild-type) and blue (LI to IV mutant) dotted lines; water molecules are shown as red (wild-type) and cyan (LI to IV mutant) spheres. d) Space-filling PyMol diagram showing the three additional pocket water molecules (cyan) in the RAD/LI to IV crystal structure.

Ser126, the main-chain carbonyls of Phe30 and Phe124, and the side-chain amine of Asn37 (Figure 2 and Figure 3). Additionally, the water molecule that interacts directly with Asn37 is also now forming a hydrogen bond to the O4-hydroxyl of RAD (Figure 2 and Figure 4).

These three additional waters are absent from the corresponding co-crystal structures of either RAD or ADP bound within the wild-type Hsp82 N-terminal domain (*17, 19*). In the RAD/LI to IV Hsp82 co-crystal structure, their presence will render the environment of the bound RAD less hydrophobic. This will reduce the affinity for RAD by disfavoring the binding of the RAD chlorine atom. This new network of hydrogen-bonded waters is also apparent in the ADP/LI to IV Hsp82 co-crystal structure (Figure 3 and Figure 4). However as the purine

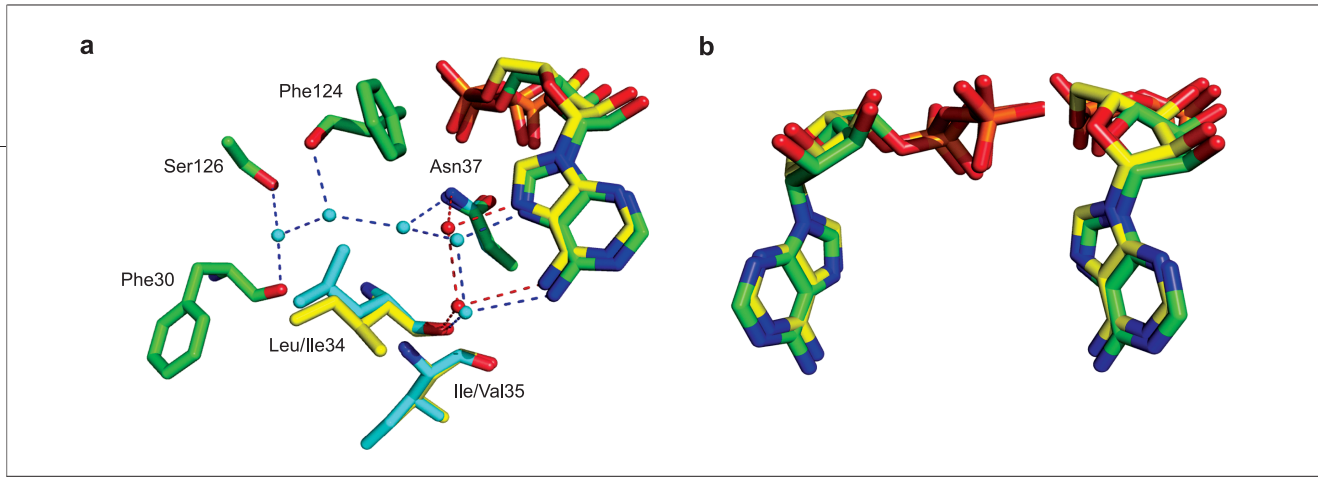

Figure 3. ADP binding to the wild-type and the L34I,I35V mutant N-terminal domain of yeast Hsp82. a) PyMol diagrams showing the interactions of ADP bound within the wild-type and mutant (L34I,I35V) N-terminal domain of Hsp82. ADP is shown in yellow (wild-type structure) and green (LI to IV mutant structure). Amino acid residues from wild-type Hsp90 are shown in cyan, and those from the LI to IV mutant are shown in green, except for the residues representing the mutation LI to IV, which are shown in yellow. Hydrogen bonds are shown as red (wild-type) and blue dotted lines (LI to IV mutant); water molecules are shown as red (wild-type) and cyan spheres (LI to IV mutant). b) Two orthogonal views of the superimposition of ADP from the co-crystal structures of wild-type and LI to IV mutant forms of Hsp82.

base of ADP does not present a hydrophobic group at the position equivalent to where RAD presents its chlorine atom, this sequence change has a much smaller effect on the affinity for AMP analogues (Table 1). With GdA, however, the LI to IV co-crystal structure reveals a different picture altogether (Figure 3 and Supplementary Figure S2). The water molecules in immediate interaction with Asn37 and the carbamate nitrogen of GdA are too close to accommodate the new water molecule network of the RAD/LI to IV Hsp82 structure. Consequently these additional water molecules are not apparent in the GdA/LI to IV Hsp82 co-crystal structure and the binding affinity for GdA is effectively unchanged (Table 1).

These structures indicate in atomic detail how RAD binding by Hsp82 is compromised by L34I, the amino acid substitution that, inserted in this yeast Hsp90, is able to recreate the lowered affinity for RAD displayed by Hsp90 of the RAD-producing fungus *H. fuscoatra* (Table 1).

Highly selective Hsp90 inhibitors act by docking within the N-terminal nucleotide binding site of Hsp90. *In vivo* their administration prevents the formation of the mature Hsp90:client multiprotein complex, this in turn causing a ubiquitin ligase (*e.g.*, CHIP) to be recruited to this complex and the client protein to be targeted for degradation *via* the ubiquitin-proteasome pathway (*1, 3–5*). Amino acid residues that facilitate the bonding of ATP, GdA, RAD, or synthetic Hsp90 inhibitor drugs within this nucleotide binding site (*9, 17–22*) are highly conserved in Hsp90-family proteins (*15*). There has therefore been considerable uncertainty as to whether any *in vivo* resistance to Hsp90 inhibitors could arise through their mutation. Changes to these residues would generally be predicted to compromise ATP binding or hydrolysis, with loss of the essential chaperone function of Hsp90. Despite this, we show in this study that nature has evolved a form of Hsp90 that has a substantially lowered affinity for RAD, the most potent natural product inhibitor of Hsp90 discovered to date (*19*), yet still retains ATP binding and ATPase activity (Table 1).

Possession of this Hsp90 with a weakened affinity for RAD most probably serves to provide *H. fuscoatra* with a degree of protection against its own antibiotic production. High-level RAD production is a feature of a number of the fungi that inhabit the rhizosphere of plants (*26*), genes of RAD biosynthesis having recently been characterized from two of these species (*Pochonia chlamydosporia* (*27*) and *Chaetomium chiversii* (*28*)). The RAD-producing fungus studied here, *H. fuscoatra*, has previously attracted interest as a possible agent for the biocontrol of important plant-pathogenic fungi (*e.g.*, *Phytophthora* spp. and *Aspergillus flavus*), as a mycoparasite that infects the sclerotia of these plant pathogens in soil (*14*).

This study identifies the main cause of the reduction in RAD binding by *H. fuscoatra* Hsp90 as being the substitution of a normally conserved leucine within the nucleotide binding pocket by isoleucine. Inserted into the Hsp82 of yeast, this conservative leucine to isoleucine change not only recreated the lowered affinity for RAD displayed by purified *H. fuscoatra* Hsp90 *in vitro* (Table 1) but also generated substantial resistance to RAD *in vivo* (Figure 1, panel d). It did not, however, appreciably affect the binding of GdA, a natural product inhibitor of Hsp90 that is derived not from fungi but from *Streptomyces hygroscopicus*. Co-crystal structures reveal that this leucine to isoleucine substitution causes the binding of additional water molecules adjacent to

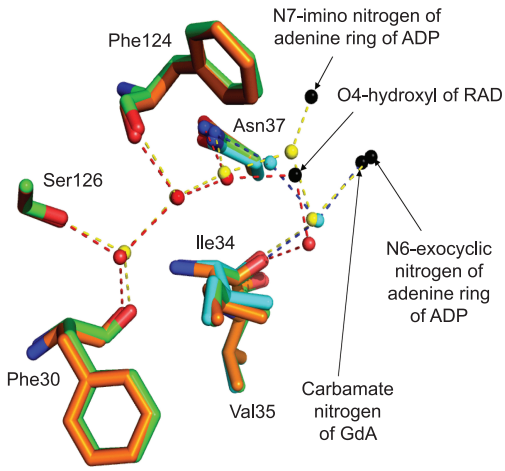

Figure 4. Comparison of the interactions made by RAD, GdA, and ADP with the LI to IV mutant Hsp82. Amino acid residues are shown in green (RAD co-crystal structure), cyan (GdA structure), and orange (ADP structure). Water molecules are shown as red (RAD structure), cyan (GdA structure), and yellow spheres (ADP structure). Hydrogen bonds are shown as red (RAD structure), blue (GdA structure), and yellow dotted lines (ADP structure). Atoms shown as black spheres are those of RAD, GdA, and ADP that engage in immediate interactions with the water molecules in immediate proximity to I34 and V35. Note that the networks of hydrogen bonds that are formed upon binding of RAD and ADP are similar but not completely identical. The presence of these water molecules interacting with Phe30, Asn37, Phe124, and Ser126 is incompatible with the GdA mode of binding.

RAD but not GdA when these inhibitors are bound within the nucleotide binding site of Hsp82 (Figure 2 and Figure 4; Supplementary Figure S2). As this increase in hydration will disfavor the binding of the RAD chlorine, these structures provide a plausible explanation as to how the leucine to isoleucine substitution lowers the affinity for RAD (Table 1).

The cytosolic Hsp90s that are major targets of cancer drug therapy, Hsp90α and Hsp90β, are encoded by just three genes in the human genome (*29*). The issue of whether drug resistance could be acquired by Hsp90 mutation is therefore a pertinent one. Clinical trials of Hsp90 inhibitors as anticancer agents are at present at too preliminary a stage for any acquired resistance to Hsp90 inhibitors to have been uncovered, let alone unraveled at the molecular level. Also, no RAD analogue has yet entered clinical trials, although inhibitors based on the interactions of RAD (*e.g.*, the 4,5-diarylisoxazole NVP-AUY922 (*9, 10*) and the purine BIIB021) are now in the clinic (*8*). This study reveals that it is possible for resistance to an Hsp90 inhibitor to arise through a small structural alteration to Hsp90. Furthermore, as the leucine to isoleucine change identified here compromises the binding of RAD but not GdA, it also reveals that a resistance-generating mutation in Hsp90 need not affect all modes of Hsp90 inhibitor binding identically. Such a finding strongly reinforces the case for the development of a clinical armamentarium of several, structurally diverse Hsp90 inhibitors.

METHODS

***E. coli* Expression of His_6-Tagged Yeast Hsp82.** pRSETA (Invitrogen)-based vectors for *E. coli* expression of His_6-tagged full-length Hsp82 (pRSETA-p90) and the 1–221 fragment of Hsp82 were as described previously (*16, 17*).

***E. coli* Expression of His_6-Tagged *H. fuscoatra* Hsp90.** The full length Hsp90 gene of *H. fuscoatra* isolate NRRL22980 (*HfHsp90*) was PCR-amplified from genomic DNA using primers GGA TCCATGGCTGAGACCTTCGAGTT and GCGGCCGCTTAGTCAACCTCCT CCATGG and then inserted into vector pCR-Blunt II-TOPO using the Zero Blunt TOPO PCR Cloning Kit (Invitrogen). Subsequently the single intron was deleted in a single PCR reaction, using the overlapping primers TATGACCAAGGCTGACCTCGTCAACAA and TT GTTGACGAGGTCAGCCTTGGTCATA and the above genomic DNA-derived *HfHsp90* clone as template. Sequencing confirmed that the gene obtained this way (2109bp) was now encoded an intronless, continuous ORF of 702 amino acids. This was reamplified using primers GCTAGCGCTGAGACCTTCGAGTTCCAG and TTAGTCAACCTCCTCCATGGC. The resulting PCR product was then digested with *Nhe*1 and *Eco*R1 and inserted into *Nhe*1 and *Eco*R1-cleaved pRSETA, so as to generate vector pRSETA-HfHsp90 for the *E. coli* expression of His_6-tagged *H. fuscoatra* Hsp90.

Mutagenesis and Yeast Strain Construction. Mutations were generated in the above pRSETA-based vectors using the QuikChange mutagenesis system (Stratagene) and confirmed by dye-terminator sequencing. Yeasts bearing vectors for *HSC82* promoter-directed expression of either Hsp82 or *H. fuscoatra* Hsp90 were generated by recombinational cloning in *S. cerevisiae* strain PP30pdr5Δ[pHSC82], a *PDR5* deletion version of PP30[pHSC82] (MAT**a** *trp1-289, leu2-3,112, his3-200,ura3-52, ade2-101^{oc}, lys2-801^{am}, hsc82ΔkanMX4, hsp82ΔkanMX4* [pHSC82] (*23*)). Initially, PCR products were generated comprising a Hsp90 gene with 40bp terminal homologies to the sequences either side of the *Pst*1 site on plasmid pHSC82prom (*30*). Hsp82-encoding genes were amplified using the appropriate wild-type or mutant pRSETA-Hsp82 template and primers: AC AGAACCAATAGAAAAATAGAATCATTCTGAAAT*ATGGCTAGTGAAACT TTTG* and CATAAATCATAAGAAATTCGCCCGGAATTAGCTTGG*CTAATC TACCTCTTCCATTTCGG* (homology to plasmid pHSCprom in italics; start and stop codons underlined); *H. fuscoatra* Hsp90 genes were amplified using the appropriate pRSETA-HfHsp90 template

and primers: ACGCTACAGAACCAATAGAAAATAGAATCATTCTGAAA T*ATG*GCTGAGACCTTCGAGTTCCAGG and AAATCATAAACATAAGAAA TTCGCCCGGAATTAGCTTGG*TTA*GTCAACCTCCTCCATGGCGCT (homology to plasmid pHSCprom in italics; start and stop codons underlined). Hsp82 or *H. fuscoatra* Hsp90-expressing yeasts were then created by transforming PP30pdr5Δ[pHSC82] with these PCR-generated genes and *Pst1*-linearized pHSC82prom. Transformants selected on leucine-minus plates were then cured of their original *URA3* plasmid pHSC82 by restreaking the cells onto 5-fluoroorotic acid plates (*30*), mutations in their remaining Hsp90 gene then being confirmed by PCR amplification and dye-terminator sequencing.

Total cell protein was extracted from 30 °C YPDA (2% (w/v) glucose, 2% bactopeptone, 1% yeast extract, 20 mg L^{-1} adenine) cultures, separated on 12.5% SDS gels, and analyzed for Hsp90 levels by Western blotting using a rabbit polyclonal antiserum raised against the 300–704 fragment of *S. cerevisiae* Hsp82, an antiserum that efficiently recognizes the Hsp90 of diverse fungal species (ref 30 and unpublished data).

Yeast Stress Sensitivity Analysis. For agar growth, serial dilutions of overnight YPDA cultures were then pronged onto YPDA 1.5% agar plates, the plates being grown under the conditions stated in the figure legends. Analysis of HSE-lacZ reporter gene expression was as previously described (*31*).

Measurements of Inhibitor Sensitivity. The inhibitory effects of increasing RAD and GdA on yeast growth were determined essentially as in earlier studies (*25, 31*). RAD and GdA were prepared as 5 or 2.8 mg mL^{-1} stock solutions in dimethylsulfoxide (DMSO), respectively, and then added to autoclaved yeast media. For liquid growth at 28 °C, overnight synthetic defined (SD) complete medium (*32*) cultures were diluted in SD to an optical density at 595 nm of 0.05 and transferred to 96-well microtiter plates (150 μL per well) in the presence of increasing levels of RAD, GdA, or vehicle DMSO.

Hsp90 Preparation, Assay of the Intrinsic ATPase, ITC Measurements, and Structure Determination. The expression, purification, and crystallization of the N-terminal domain of yeast Hsp90 have been described previously (*33*). The Hsp90 ATPase assay, ITC measurements, and K_d determinations of heats of interaction were as previously described (*17, 34, 35*). Briefly, 14 aliquots of 20 μL of 70 μM RAD, 120 μM GdA, or 1 mM AMP-PNP were injected into 6, 10, or 50 μM recombinant full-length wild-type or mutant yeast or *H. fuscoatra* Hsp90, respectively, at 30 °C in 20 mM Tris (pH 7.5), 1 mM EDTA, 5 mM NaCl, and 2% DMSO. For structure determination and refinement tetragonal crystals of the N-terminal domain (amino acid residues 1–221) of yeast Hsp82, either native or complexed with either ATPγS, RAD, or GdA, were grown and harvested as previously described (*17, 19*). The crystals were stabilized for freezing in a solution containing 30% glycerol, 90 mM ammonium sulfate, 45 mM sodium succinate (pH 5), and 13.5% poly(ethylene glycol) methyl ester 550. Diffraction data were collected from crystals frozen at 100 K on Station I03 at the Diamond Light Source. The RAD data set would not merge well in $P4_322$ and was finally merged in $P222_1$. The structures were determined by molecular replacement with the coordinates of the native tetragonal crystal form of the yeast Hsp90 N-domain (Protein Data Bank code 1AH6). Refinement was carried out using refmac (*36*), and manual rebuilding was performed in COOT (*37*). All other programs used were part of the CCP4 suite (*38*).

Acknowledgment: We are indebted to Andrew Truman and Mehdi Mollapour for their assistance in the early stages of this work and also to an anonymous referee for their suggestions. This work was supported by Cancer Research UK project (C28248/A9058) programme (C309/A8274) and Infrastructure Support (C302/A7803) grants; a Wellcome Trust Programme Grant (080041); a BBSRC studentship (J.M.N.); and the Diamond Light Source. P.W. is a Cancer Research UK Life Fellow.

Supporting Information Available: This material is available free of charge *via* the Internet at http://pubs.acs.org.

REFERENCES

1. Scroggins, B. T., Robzyk, K., Wang, D., Marcu, M. G., Tsutsumi, S., Beebe, K., Cotter, R. J., Felts, S., Toft, D., Karnitz, L., Rosen, N., and Neckers, L. (2007) An acetylation site in the middle domain of Hsp90 regulates chaperone function, *Mol. Cell 25*, (1), 151–159.
2. Pearl, L. H., Prodromou, C., and Workman, P. (2008) The Hsp90 molecular chaperone: an open and shut case for treatment, *Biochem. J. 410*, (3), 439–453.
3. McDonald, E., Jones, K., Brough, P. A., Drysdale, M. J., and Workman, P. (2006) Discovery and development of pyrazole-scaffold Hsp90 inhibitors, *Curr. Top. Med. Chem. 6*, (11), 1193–1203.
4. Sharp, S., and Workman, P. (2006) Inhibitors of the HSP90 molecular chaperone: current status, *Adv. Cancer Res. 95*, 323–348.
5. Neckers, L. (2007) Heat shock protein 90: the cancer chaperone, *J. Biosci. 32*, (3), 517–530.
6. Kamal, A., Thao, L., Sensintaffar, J., Zhang, L., Boehm, M. F., Fritz, L. C., and Burrows, F. J. (2003) A high-affinity conformation of Hsp90 confers tumour selectivity on Hsp90 inhibitors, *Nature 425*, (6956), 407–410.
7. Workman, P., Burrows, F., Neckers, L., and Rosen, N. (2007) Drugging the cancer chaperone HSP90: combinatorial therapeutic exploitation of oncogene addiction and tumor stress, *Ann. N.Y. Acad. Sci. 1113*, 202–216.
8. Taldone, T., Gozman, A., Maharaj, R., and Chiosis, G. (2008) Targeting Hsp90: small-molecule inhibitors and their clinical development, *Curr. Opin. Pharmacol. 8*, (4), 370–374.
9. Brough, P. A., Aherne, W., Barril, X., Borgognoni, J., Boxall, K., Cansfield, J. E., Cheung, K. M., Collins, I., Davies, N. G., Drysdale, M. J., Dymock, B., Eccles, S. A., Finch, H., Fink, A., Hayes, A., Howes, R., Hubbard, R. E., James, K., Jordan, A. M., Lockie, A., Martins, V., Massey, A., Matthews, T. P., McDonald, E., Northfield, C. J., Pearl, L. H., Prodromou, C., Ray, S., Raynaud, F. I., Roughley, S. D., Sharp, S. Y., Surgenor, A., Walmsley, D. L., Webb, P., Wood, M., Workman, P., and Wright, L. (2008) 4,5-Diarylisoxazole Hsp90 chaperone inhibitors: potential therapeutic agents for the treatment of cancer, *J. Med. Chem. 51*, (2), 196–218.
10. Eccles, S. A., Massey, A., Raynaud, F. I., Sharp, S. Y., Box, G., Valenti, M., Patterson, L., de Haven Brandon, A., Gowan, S., Boxall, F., Aherne, W., Rowlands, M., Hayes, A., Martins, V., Urban, F., Boxall, K., Prodromou, C., Pearl, L., James, K., Matthews, T. P., Cheung, K. M., Kalusa, A., Jones, K., McDonald, E., Barril, X., Brough, P. A., Cansfield, J. E., Dymock, B., Drysdale, M. J., Finch, H., Howes, R., Hubbard, R. E., Surgenor, A., Webb, P., Wood, M., Wright, L., and Workman, P. (2008) NVP-AUY922: a novel heat shock protein 90 inhibitor active against xenograft tumor growth, angiogenesis, and metastasis, *Cancer Res. 68*, (8), 2850–2860.
11. Piper, P. W., Millson, S. H., Mollapour, M., Panaretou, B., Siligardi, G., Pearl, L. H., and Prodromou, C. (2003) Sensitivity to Hsp90-targeting drugs can arise with mutation to the Hsp90 chaperone, cochaperones and plasma membrane ATP binding cassette transporters of yeast, *Eur. J. Biochem. 270*, 4689–4695.
12. Holmes, J. L., Sharp, S. Y., Hobbs, S., and Workman, P. (2008) Silencing of HSP90 cochaperone AHA1 expression decreases client protein activation and increases cellular sensitivity to the HSP90 inhibitor 17-allylamino-17-demethoxygeldanamycin, *Cancer Res. 68*, (4), 1188–1197.
13. Forafonov, F., Toogun, O. A., Grad, I., Suslova, E., Freeman, B. C., and Picard, D. (2008) p23/Sba1p protects against Hsp90 inhibitors independently of its intrinsic chaperone activity, *Mol. Cell. Biol. 28*, 3446–3456.

14. Wicklow, D. T., Joshi, B. K., Gamble, W. R., Gloer, J. B., and Dowd, P. F. (1998) Antifungal metabolites (monorden, monocillin IV, and cerebrosides) from *Humicola fuscoatra*Traaen NRRL 22980, a mycoparasite of *Aspergillus flavus* sclerotia, *Appl. Environ. Microbiol. 64*, (11), 4482–4484.
15. Chen, B., Zhong, D., and Monteiro, A. (2006) Comparative genomics and evolution of the HSP90 family of genes across all kingdoms of organisms, *BMC Genomics 7*, 156.
16. Prodromou, C., Panaretou, B., Chohan, S., Siligardi, G., O'Brien, R., Ladbury, J. E., Roe, S. M., Piper, P. W., and Pearl, L. H. (2000) The ATPase cycle of Hsp90 drives a molecular 'clamp' *via* transient dimerization of the N-terminal domains, *EMBO J. 19*, 4383–4392.
17. Prodromou, C., Roe, S. M., O'Brien, R., Ladbury, J. E., Piper, P. W., and Pearl, L. H. (1997) Identification and structural characterization of the ATP/ADP-binding site in the Hsp90 molecular chaperone, *Cell 90*, (1), 65–75.
18. Stebbins, C. E., Russo, A. A., Schneider, C., Rosen, N., Hartl, F. U., and Pavletich, N. P. (1997) Crystal structure of an Hsp90-geldanamycin complex: targeting of a protein chaperone by an antitumor agent, *Cell 89*, (2), 239–250.
19. Roe, S. M., Prodromou, C., O'Brien, R., Ladbury, J. E., Piper, P. W., and Pearl, L. H. (1999) Structural basis for inhibition of the Hsp90 molecular chaperone by the antitumor antibiotics radicicol and geldanamycin, *J. Med. Chem. 42*, (2), 260–266.
20. Cheung, K. M., Matthews, T. P., James, K., Rowlands, M. G., Boxall, K. J., Sharp, S. Y., Maloney, A., Roe, S. M., Prodromou, C., Pearl, L. H., Aherne, G. W., McDonald, E., and Workman, P. (2005) The identification, synthesis, protein crystal structure and *in vitro* biochemical evaluation of a new 3,4-diarylpyrazole class of Hsp90 inhibitors, *Bioorg. Med. Chem. Lett. 15*, (14), 3338–3343.
21. Proisy, N., Sharp, S. Y., Boxall, K., Connelly, S., Roe, S. M., Prodromou, C., Slawin, A. M., Pearl, L. H., Workman, P., and Moody, C. J. (2006) Inhibition of Hsp90 with synthetic macrolactones: synthesis and structural and biological evaluation of ring and conformational analogs of radicicol, *Chem. Biol. 13*, (11), 1203–1215.
22. Sharp, S. Y., Boxall, K., Rowlands, M., Prodromou, C., Roe, S. M., Maloney, A., Powers, M., Clarke, P. A., Box, G., Sanderson, S., Patterson, L., Matthews, T. P., Cheung, K. M., Ball, K., Hayes, A., Raynaud, F., Marais, R., Pearl, L., Eccles, S., Aherne, W., McDonald, E., and Workman, P. (2007) *In vitro* biological characterization of a novel, synthetic diaryl pyrazole resorcinol class of heat shock protein 90 inhibitors, *Cancer Res. 67*, (5), 2206–2216.
23. Panaretou, B., Prodromou, C., Roe, S. M., O'Brien, R., Ladbury, J. E., Piper, P. W., and Pearl, L. H. (1998) ATP binding and hydrolysis are essential to the function of the Hsp90 molecular chaperone *in vivo*, *EMBO J. 17*, (16), 4829–4836.
24. Borkovich, K. A., Farrelly, F. W., Finkelstein, D. B., Taulien, J., and Lindquist, S. (1989) hsp82 is an essential protein that is required in higher concentrations for growth of cells at higher temperatures, *Mol. Cell. Biol. 9*, (9), 3919–3930.
25. Piper, P. W., Panaretou, B., Millson, S. H., Truman, A., Mollapour, M., Pearl, L. H., and Prodromou, C. (2003) Yeast is selectively hypersensitised to heat shock protein 90 (Hsp90)-targetting drugs with heterologous expression of the human Hsp90, a property that can be exploited in screens for new Hsp90 chaperone inhibitors, *Gene 302*, (1–2), 165–170.
26. Turbyville, T. J., Wijeratne, E. M., Liu, M. X., Burns, A. M., Seliga, C. J., Luevano, L. A., David, C. L., Faeth, S. H., Whitesell, L., and Gunatilaka, A. A. (2006) Search for Hsp90 inhibitors with potential anticancer activity: isolation and SAR studies of radicicol and monocillin I from two plant-associated fungi of the Sonoran desert, *J. Nat. Prod. 69*, (2), 178–184.
27. Reeves, C. D., Hu, Z., Reid, R., and Kealey, J. T. (2008) Genes for the biosynthesis of the fungal polyketides hypothemycin from *Hypomyces subiculosus* and radicicol from *Pochonia chlamydosporia*, *Appl. Environ. Microbiol. 74*, (16), 5121–5129.
28. Wang, S., Xu, Y., Maine, E. A., Wijeratne, E. M., Espinosa-Artiles, P., Gunatilaka, A. A., and Molnar, I. (2008) Functional characterization of the biosynthesis of radicicol, an Hsp90 inhibitor resorcylic acid lactone from *Chaetomium chiversii*, *Chem. Biol. 15*, (12), 1328–1338.
29. Chen, B., Piel, W. H., Gui, L., Bruford, E., and Monteiro, A. (2005) The HSP90 family of genes in the human genome: insights into their divergence and evolution, *Genomics 86*, (6), 627–637.
30. Panaretou, B., Sinclair, K., Prodromou, C., Johal, J., Pearl, L., and Piper, P. W. (1999) The Hsp90 of *Candida albicans* can confer Hsp90 functions in *Saccharomyces cerevisiae*: a potential model for the processes that generate immunogenic fragments of this molecular chaperone in *C. albicans* infections, *Microbiology 145*, (Pt 12), 3455–3463.
31. Millson, S. H., Truman, A. W., Rácz, A., Hu, B., Nuttall, J., Mollapour, M., Söti, C., and Piper, P. W. (2007) Expressed as the sole Hsp90 in yeast, the α and β isoforms of human Hsp90 differ in their capacities to activate certain client proteins, while only Hsp90β sensitizes cells to the Hsp90 inhibitor radicicol, *FEBS J. 274*, 4453–4463.
32. Adams, A.; Gottschling, D. E.; Kaiser, C. A.; Stearns, T. (1997) *Methods in Yeast Genetics*, Cold Spring Harbor Laboratory Press, Cold Spring Harbor, NY.
33. Prodromou, C., Piper, P. W., and Pearl, L. H. (1996) Expression and crystallization of the yeast Hsp82 chaperone, and preliminary X-ray diffraction studies of the amino-terminal domain, *Proteins 25*, (4), 517–522.
34. Prodromou, C., Siligardi, G., O'Brien, R., Woolfson, D. N., Regan, L., Panaretou, B., Ladbury, J. E., Piper, P. W., and Pearl, L. H. (1999) Regulation of Hsp90 ATPase activity by tetratricopeptide repeat (TPR)-domain co-chaperones, *EMBO J. 18*, (3), 754–762.
35. Panaretou, B., Siligardi, G., Meyer, P., Maloney, A., Sullivan, J. K., Singh, S., Millson, S. H., Clarke, P. A., Naaby-Hansen, S., Stein, R., Cramer, R., Mollapour, M., Workman, P., Piper, P. W., Pearl, L. H., and Prodromou, C. (2002) Activation of the ATPase activity of Hsp90 by AHA1 and other co-chaperones, *Mol. Cell 10*, 1307–1318.
36. Murshudov, G. N., Vagin, A. A., and Dodson, E. J. (1997) Refinement of macromolecular structures by the maximum-likelihood method, *Acta Crystallogr., Sect. D: Biol. Crystallogr. 53*, (Pt 3), 240–255.
37. Emsley, P., and Cowtan, K. (2004) Coot: model-building tools for molecular graphics, *Acta Crystallogr., Sect. D: Biol. Crystallogr. 60*, (Pt 12 Pt 1), 2126–2132.
38. Krissinel, E. B., Winn, M. D., Ballard, C. C., Ashton, A. W., Patel, P., Potterton, E. A., McNicholas, S. J., Cowtan, K. D., and Emsley, P. (2004) The new CCP4 Coordinate Library as a toolkit for the design of coordinate-related applications in protein crystallography, *Acta Crystallogr., Sect. D: Biol. Crystallogr. 60*, (Pt 12 Pt 1), 2250–2255.